



ELSEVIER

Contents lists available at SciVerse ScienceDirect

Organic Electronics

journal homepage: www.elsevier.com/locate/orgel

Solution-processed near-infrared polymer photodetectors with an inverted device structure

Xilan Liu, Hangxing Wang, Tingbin Yang, Wei Zhang, I-Fan Hsieh, Stephen Z.D. Cheng, Xiong Gong*

College of Polymer Science and Polymer Engineering, The University of Akron, Akron, OH 44325, United States

ARTICLE INFO

Article history:

Received 29 May 2012

Received in revised form 28 July 2012

Accepted 17 August 2012

Available online 6 September 2012

Keywords:

Semiconducting polymer

Photodetectors

Inverted device structure

Infrared spectral response

ABSTRACT

Solution-processed near-infrared polymer photodetectors with an inverted device structure were designed and fabricated. By introducing ZnO_x and MoO_3 as an electron extraction layer and a hole extraction layer, respectively, the asymmetric characteristics of the inverted polymer photodetectors was constructed. Operating at room temperature, the inverted polymer photodetectors exhibited the detectivity over $10^{12} \text{ cm Hz}^{1/2}/\text{W}$ from 400 to 850 nm, resulting from the enhanced photocurrent and reduced dark current induced by fabricating photoactive layer from solution with processing additive 1,8-diiodooctane. These device performances were comparable to those of inorganic counterparts.

© 2012 Elsevier B.V. All rights reserved.

In the past decade, polymer photodetectors (PDs) have been extensively investigated due to their low-cost processing and high performance at room temperature for various potential applications [1–5]. In particular, with the development of new narrow bandgap conjugated polymers, better control of nanoscale morphology of electron donor (D)/electron acceptor (A) networks and introduction of functional buffer layers in the device layout, the detectivity of solution-processed polymer PDs with spectral response from ultraviolet (UV) to near infrared (NIR) have reached 10^{13} Jones (1 Jones = $1 \text{ cm Hz}^{1/2}/\text{W}$) [6–12].

Currently, ongoing research are mainly focused on polymer PDs with a conventional device structure, in which the bulk heterojunction (BHJ) composite of semiconducting polymers (D) and fullerene derivatives (A) are sandwiched between poly(3,4-ethylenedioxythiophene):poly(styrenesulfonate) (PEDOT:PSS) modified indium tin oxides (ITO) anode and low-work-function cathode (e.g. Al). In the conventional device structure, the acid PEDOT:PSS etches ITO and degrades the performance of devices [13,14]. The top

air-sensitive cathodes, including relatively stable Al, are inherently flawed giving poor long-term stability. Moreover, the availability of low-work-function metal inks is unlikely possible; Hence, continuous low-cost printing technology for depositing large-area Al cathode remains an issue. In order to circumvent above problems, inverted device structures have been recently developed. In the inverted device architecture, the polarity of the device is reversed by using high-work-function metals, such as Ag or Au, which are stable in air and can be printed from paste inks, as the anode and ITO as the cathode. The elimination of acid PEDOT:PSS in the inverted device structure implies the devices can possess good stability.

Inverted polymer solar cells (PSCs) with comparable efficiency and enhanced stability have been reported [15–22]. However, few inverted polymer PDs has been demonstrated [23]. In this work, we report inverted polymer PDs with a device structure in which ITO acts as the cathode and Ag as the anode. By inserting ZnO_x and MoO_3 as an electron extraction layer and a hole extraction layer, respectively, the asymmetric characteristics of the photodiodes and the detection function of the device were accomplished. The influence of processing additive 1,8-diiodooctane (DIO) in fabrication

* Corresponding author. Fax: +1 (330) 972 2339.

E-mail address: xgong@uakron.edu (X. Gong).

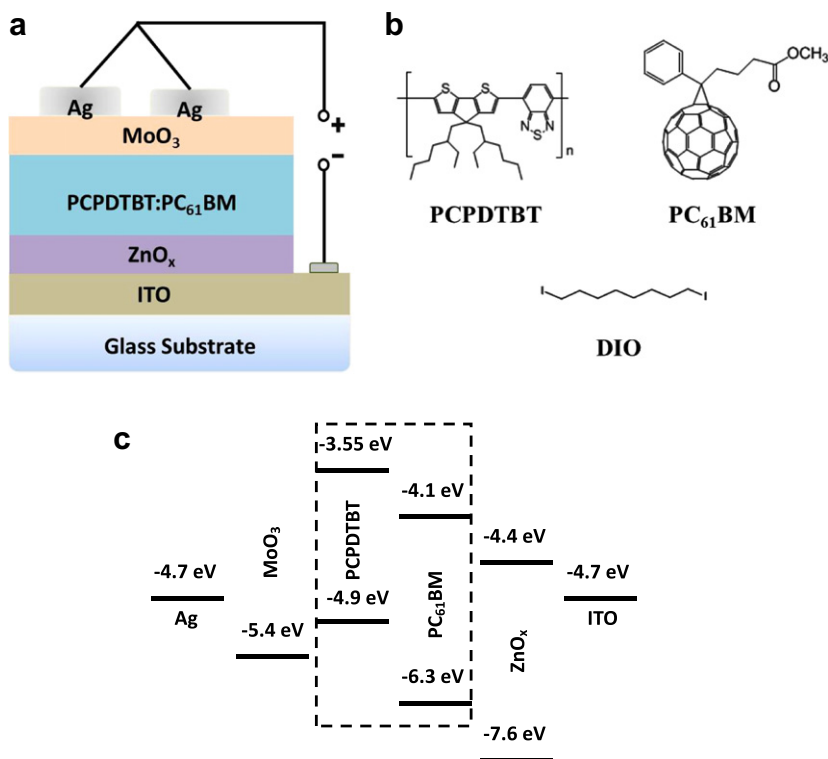


Fig. 1. (a) Device architecture of the inverted polymer photodetectors; (b) molecular structures of PCPDTBT, PC₆₁BM and DIO; (c) energy levels of PCPDTBT, PC₆₁BM, ZnO_x and MoO₃, with the workfunctions of ITO and Ag.

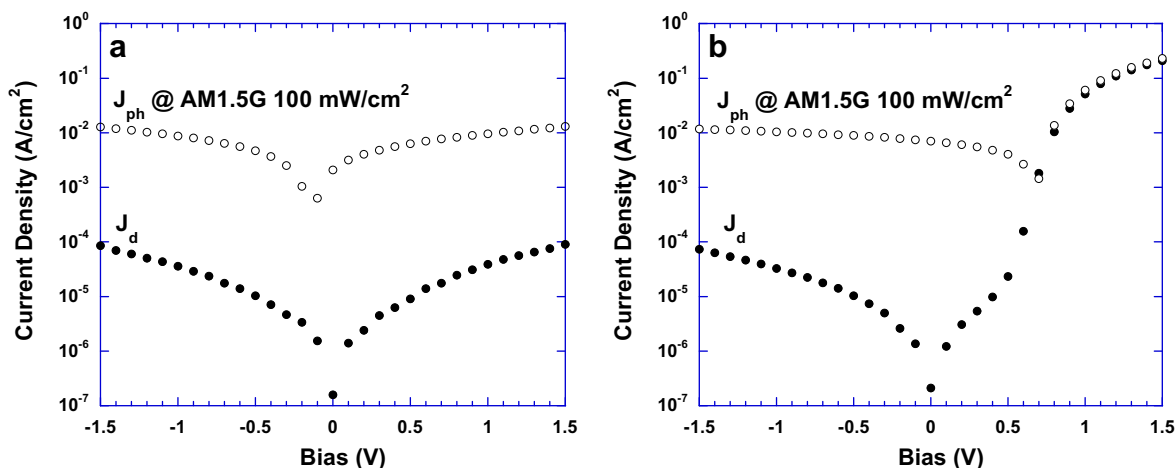


Fig. 2. (a) J - V characteristics of the polymer photodetectors without ZnO_x and MoO₃ buffer layers; (b) J - V characteristics of the polymer photodetectors with ZnO_x and MoO₃ buffer layers.

of photoactive layer on the performance of inverted polymer PDs was also investigated.

The inverted polymer PDs were built up with the structures of ITO/PCPDTBT:PC₆₁BM/Ag and ITO/ZnO_x/PCPDTBT:PC₆₁BM/MoO₃/Ag, where PCPDTBT was poly[2,6-(4,4-bis(2-ethylhexyl)-4H-cyclopenta[2,1-b;3,4-b']dithiophene)-alt-4,7-(2,1,3-benzothiadiazole)] and PC₆₁BM was [6,6]-phenyl C₆₁-butyric acid methyl ester. (Fig. 1a and b) present

the device architecture of the inverted polymer PDs and the molecular structures of PCPDTBT, PC₆₁BM and processing additive, DIO, respectively. The photoactive layer, PCPDTBT:PC₆₁BM, was spin cast from chlorobenzene (CB) solution composed of 8 mg mL⁻¹ PCPDTBT and 24 mg mL⁻¹ PC₆₁BM. For inverted polymer PDs with both ZnO_x and MoO₃ buffer layer, the ZnO_x layer with a thickness of approximate 35 nm was prepared prior to the photoactive layer by spin-

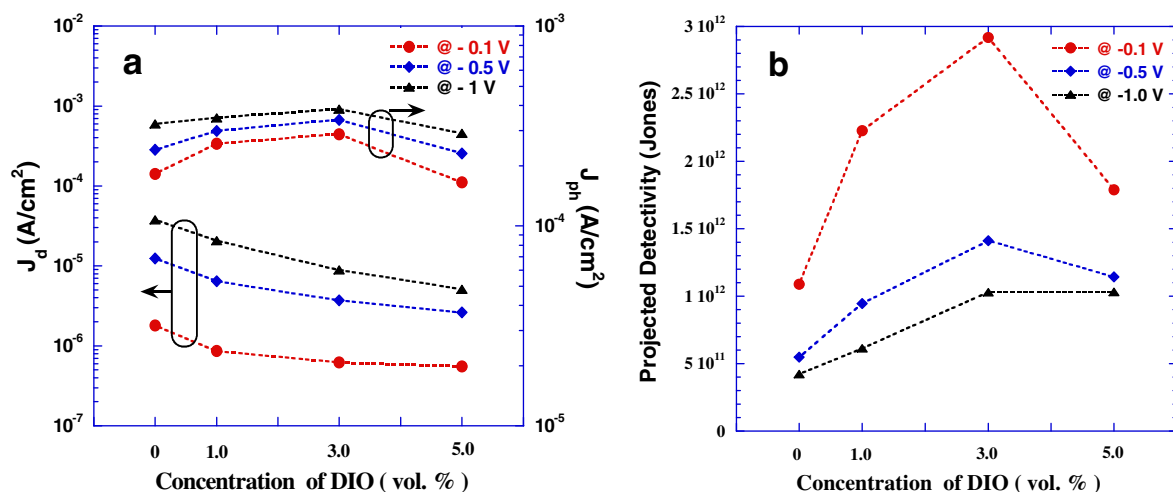


Fig. 3. (a) Dark currents and photocurrents measured under illumination of $\lambda = 800$ nm monochromatic light for the inverted polymer photodetectors processed with different concentration of DIO; (b) projected detectivity of the inverted polymer photodetectors processed with different concentration of DIO.

coating 0.5 mol L^{-1} ZnO_x precursor solution consisting of zinc acetate, ethanolamine and 2-methoxyethanol solvent on the pre-cleaned ITO/glass substrate, followed by annealing at 200°C in the air for 1 h [21]. The thin MoO_3 layer with a thickness of approximate 10 nm was vacuum deposited on the top of the photoactive layer with an evaporation rate of 0.1 \AA s^{-1} . Top electrode Ag was thermal deposited through shade mask with the effective device area of 16 mm^2 .

Fig. 1c shows the energy levels of PCPDTBT, PC_{61}BM , ZnO_x and MoO_3 , and workfunctions of ITO and Ag electrodes. Since ZnO_x is a n-type semiconductor with high electron mobility [21,24] and the valence band maximum of ZnO_x is up to -7.6 eV , ZnO_x is expected to be an electron extraction layer as well as a hole blocking layer. On the other side, MoO_3 functions as a hole extraction and electron blocking layer in the inverted polymer PDs, as it is used as an efficient anode buffer layer in organic photovoltaics [21,25–29] because of nontoxicity high stability and very deep lying electronic states [30].

The current density versus voltage (J - V) characteristics of the inverted polymer PDs are shown in (Fig. 2a and b). It was found in Fig. 2a that the inverted polymer PDs without both ZnO_x and MoO_3 buffer layers exhibited perfect symmetrical J - V characteristics, both in dark and under illumination of white light. The device behaves as a photoswitch with higher photocurrent but no built-in potential. While the inverted polymer PDs with both ZnO_x and MoO_3 buffer layers possessed a good asymmetric dark J - V curve with a

rectification ratio over 10^3 at $\pm 1 \text{ V}$. Notable photovoltaic effect with photoinduced current at open circuit and built-in potential are well observed.

To break the symmetry is an essential request for BHJ organic photovoltaic cells. Since D and A are intimately intermixed in the bulk volume, there is no intrinsic direction of the internal fields for free charges, i.e. electrons and holes have no preferred way they should move to [31,32]. Due to the similar workfunctions, ITO (-4.7 eV) cathode and Ag (-4.7 eV) anode did not provide such an electrical field, the photodiodes, such as the inverted polymer PDs without the buffer layers, showed symmetric J - V characteristics. In this case, the devices could not effectively collect photoinduced charge carriers under small bias, making it inappropriate for photon detection purpose. When ZnO_x and MoO_3 were introduced into the inverted architecture as buffer layers, symmetry breaking was constructed for the inverted polymer PDs. As a result, the detection of light could be accomplished at small reverse bias where the photo-induced charge carriers were effectively collected and photocurrent distinguished largely from the dark current. These results demonstrated that to break the symmetry of the photodiodes by the buffer layers, ZnO_x and MoO_3 , is crucial for the inverted polymer PDs.

Optimization of device performance via controlling BHJ composite morphology has been a common strategy [33]. Thermal annealing and solvent annealing have been critical for optimizing the charge separation and migration in the

Table 1

The performance of the inverted polymer photodetectors with 3.0% DIO.

Thickness ^a (nm)	J_d^b (A/cm^2)	J_{ph}^b at $\lambda = 500 \text{ nm}$ (A/cm^2)	D^{*c} at $\lambda = 500 \text{ nm}$ (Jones)	J_{ph}^b at $\lambda = 800 \text{ nm}$ (A/cm^2)	D^{*c} at $\lambda = 800 \text{ nm}$ (Jones)
150	$6.44\text{E}-6$	$3.66\text{E}-4$	$7.97\text{E}+11$	$4.14\text{E}-4$	$1.31\text{E}+12$
200	$1.43\text{E}-6$	$3.56\text{E}-4$	$1.64\text{E}+12$	$3.67\text{E}-4$	$2.47\text{E}+12$
320	$2.06\text{E}-6$	$2.52\text{E}-4$	$9.70\text{E}+11$	$2.31\text{E}-4$	$1.29\text{E}+12$

^a Thickness of active layer.

^b Photocurrent measured at bias of -0.5 V .

^c Detectivity calculated at -0.5 V .

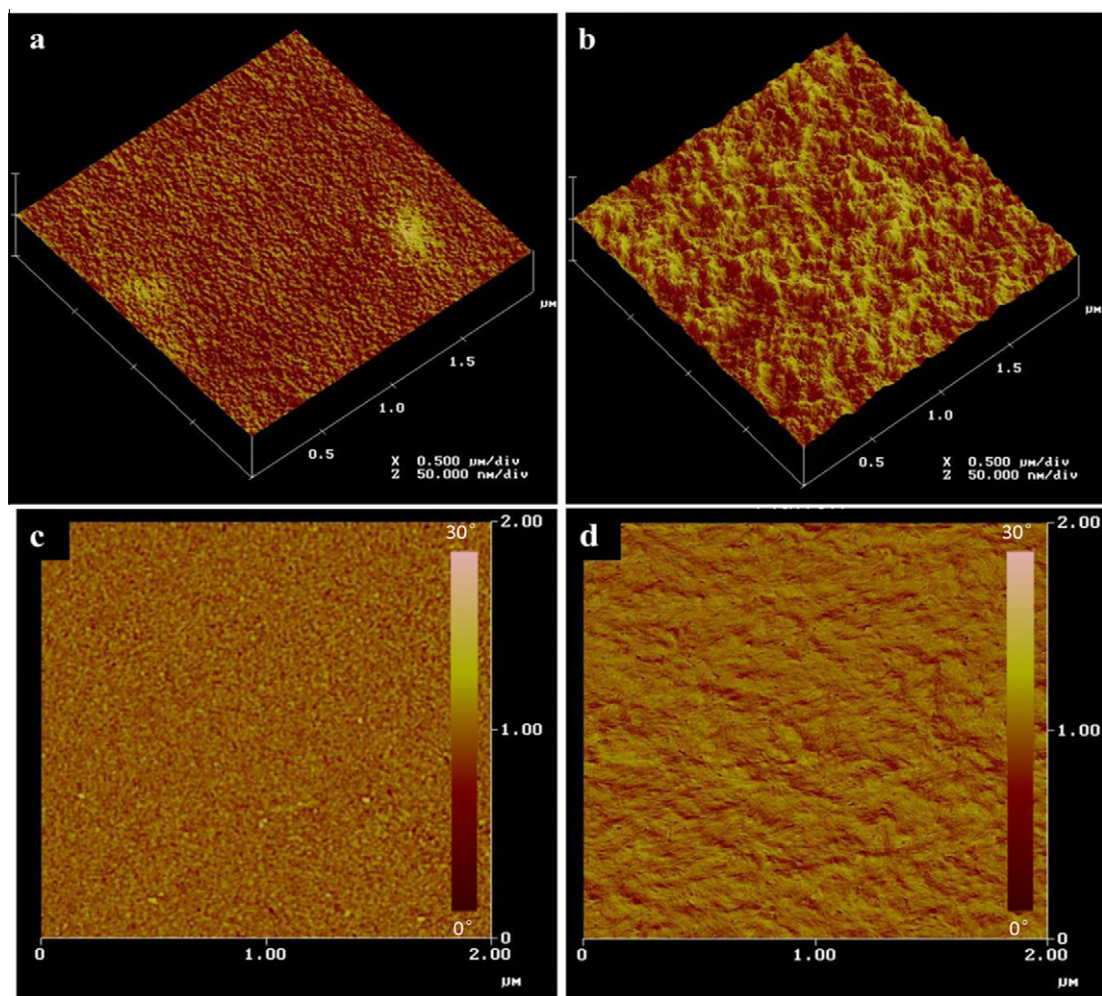


Fig. 4. AFM tapping-mode surface images of PCPDTBT:PC₆₁BM films on glass/ITO/ZnO_x. Height images of films processed without and with 3.0% DIO in (a) and (b), respectively. Phase images of films processed without and with 3.0% DIO in (c) and (d), respectively.

phase separated morphology of several BHJ blends, however, they have not been successful to improve the performance of PCPDTBT:PCBM mixture yet [34,35]. Whereas, with a small amount of processing additives, modified nanomorphology leading to a nearly doubled power conversion efficiency of PCPDTBT:PCBM PSCs has been reported [36,37]. In order to optimize the performance of the inverted polymer PDs, devices with photoactive layer of approximately 200 nm thick processed from CB solutions containing 0%, 1.0%, 3.0% and 5.0% (by volume) of DIO were investigated. Note that DIO was removed by vacuum pumping before deposition of the following layers. Fig. 3a shows the dark currents and photocurrents measured under monochromatic light at wavelength $\lambda = 800$ nm with the light intensity of 0.22 mW cm^{-2} . Under the biases of -0.1 , -0.5 and -1 V, the photocurrents were at the same magnitude, however, the highest photocurrent was observed from the inverted polymer PDs processed from CB with 3.0% of DIO. Moreover, a decreasing dark current was observed from the inverted polymer PDs processed from CB solution with increasing content of DIO. Based on

observed photocurrents and dark currents, we have calculated the detectivities of the inverted polymer PDs [10]. The detectivities of the inverted polymer PDs processed from CB solution with different concentrations of DIO were shown in Fig. 3b. The detectivities of the inverted polymer PDs were enhanced by processing active layer from CB solution with DIO. But the detectivities tended to decrease when active layer was processed with DIO beyond 3.0%. The highest detectivity, more than 10^{12} Jones, was observed from the inverted polymer PDs processed from CB solution with 3.0% of DIO.

Further device optimization has been carried out by fabricating devices of photoactive layer processed from CB solution with 3.0% of DIO with thickness of 150, 200 and 320 nm. Table 1 summarizes the detectivities of the inverted polymer PDs with different active layer thickness. It is manifested that the performance of the inverted polymer PDs is active layer thickness dependent. And the best detectivity was observed from the inverted polymer PDs with the thickness of active layer about 200 nm.

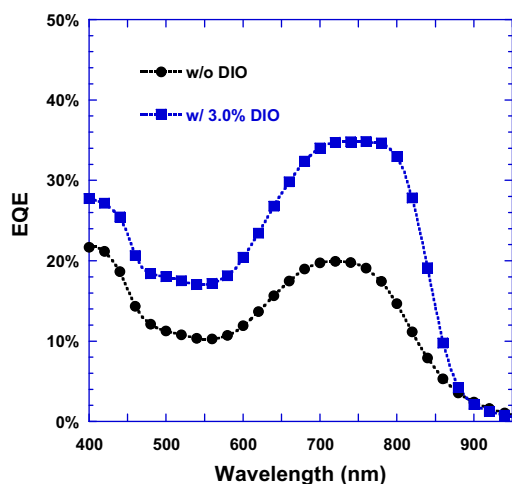


Fig. 5. EQE profiles of the inverted polymer photodetectors processed without and with 3.0% DIO.

In order to understand how processing additive DIO affects the dark current and photocurrent of inverted polymer PDs, atomic force microscopy (AFM) was used to study the film morphology of active layer. (Fig. 4a and b) show the AFM tapping-mode height images of PCPDTBT:PC₆₁BM films processed from CB solutions with and without 3.0% of DIO, respectively. A rougher film surface has been observed from the film processed from CB with DIO than that without DIO. This rough surface can ensure a strong interaction and large contact areas between the active layer and top electrode [38], resulting in high photocurrent. Moreover, the phase image of the BHJ composite film processed from CB solution with 3.0% of DIO, shown in Fig. 4d, displayed coarsened phase separation with larger length scale as compared with that without DIO, shown in Fig. 4c. This phase separation at more favorable length scale would probably constitute better bicontinuous network, thus facilitate charge transporting through BHJ composite to corresponding electrodes, resulting in enhanced photocurrent and reduced dark current due to fewer isolated domains which act as recombination centers. Besides, it was noted that the PCPDTBT:PC₆₁BM film processed from CB with 3.0% of DIO exhibited more fibril-like phase. This indicated that polymer molecules moved towards the free surface. Consequently, fullerene molecules was rich near the bottom cathode in the inverted device [39]. This proposed vertical profile of component distribution would reduce the probability of recombination at the interface between active layer and adjacent, leading to reduced dark currents.

The external quantum efficiencies (EQE) were also measured under short circuit condition. Fig. 5 shows the EQE spectra of the inverted polymer PDs processed from CB solution with and without 3.0% of DIO. The spectral response of these inverted polymer PDs are from 400 to 900 nm. The EQE profile from inverted polymer PDs processed from CB solution with 3.0% of DIO was significantly enhanced as compared with that without DIO. Moreover, the EQE profiles revealed that the responsivity of the inverted polymer PDs processed from CB solution with 3.0% of DIO have a broader peak centered at ~750 nm as

compared with those without DIO. This broadened peak suggested more ordered phases with possible improved crystallinity of polymer chains induced by DIO. This observation was similar to the effect of 1,8-octanedithiol (ODT) on PCPDTBT:PC₇₁BM films which has been evidenced by grazing incidence X-ray diffraction (GIXRD) [39].

In conclusion, inverted polymer PDs fabricated from narrow bandgap polymer PCPDTBT and PC₆₁BM have been successfully demonstrated. It was found that electron extraction layer ZnO_x and hole extraction layer MoO₃ played important roles in the performance of inverted polymer PDs. Processing additive DIO has an impact on the film morphology of photoactive layer and thus affects the device performance. Operated at room temperature, the inverted polymer PDs exhibited the detectivities greater than 10¹² - Jones from 400 to 850 nm. These results demonstrated that the NIR inverted polymer PDs are comparable to inorganic counterparts.

References

- [1] M. Ettenberg, *Adv. Imaging* 20 (2005) 29.
- [2] G. Konstantatos, I. Howard, A. Fischer, S. Hoogland, J. Clifford, E. Klem, L. Levina, E.H. Sargent, *Nature* 442 (2006) 180.
- [3] E.H. Sargent, *Adv. Mater.* 17 (2005) 515.
- [4] S. Kim, Y.T. Lim, E.G. Soltesz, A.M. de Grand, J. Lee, A. Nakayama, J.A. Parker, T. Mihaljevic, R.G. Laurence, D.M. Dor, L.H. Cohn, M.G. Bawendi, J.V. Frangioni, *Nat. Biotechnol.* 22 (2004) 93.
- [5] S.A. McDonald, G. Konstantatos, S. Zhang, P.W. Cyr, E.J.D. Klem, L. Levina, E.H. Sargent, *Nat. Mater.* 4 (2005) 138.
- [6] G. Yu, K. Pakbaz, A.J. Heeger, *Appl. Phys. Lett.* 64 (1994) 3422.
- [7] P. Schilinsky, C. Waldauf, C.J. Brabec, *Appl. Phys. Lett.* 81 (2002) 3885.
- [8] G.A. O'Brien, A.J. Quinn, D.A. Tanner, G. Redmond, *Adv. Mater.* 18 (2006) 2379.
- [9] Y. Yao, Y. Liang, V. Shrotriya, S. Xiao, L. Yu, Y. Yang, *Adv. Mater.* 19 (2007) 3979.
- [10] X. Gong, M.-H. Tong, Y. Xia, W. Cai, J.S. Moon, Y. Cao, G. Yu, C.-L. Shieh, B. Nilsson, A.J. Heeger, *Science* 325 (2009) 1665.
- [11] X. Gong, M.-H. Tong, S.H. Park, M. Liu, A.K.-Y. Jen, A.J. Heeger, *Sensors* 10 (2010) 6488.
- [12] E.-C. Chen, S.-R. Tseng, Y.-C. Chao, H.-F. Meng, C.-F. Wang, W.-C. Chen, C.-S. Hsu, S.-F. Horng, *Synth. Met.* 161 (2011) 1618.
- [13] M.P. de Jong, L.J. van Ijzendoorn, M.J.A. de Voigt, *Appl. Phys. Lett.* 77 (2000) 2255.
- [14] M. Jørgensen, K. Norrman, F.C. Krebs, *Sol. Energy Mater. Sol. Cells* 92 (2008) 686.
- [15] Y. Sahin, S. Alem, R. Bettignies, J.M. Nunzi, *Thin Solid Films* 476 (2005) 340.
- [16] G. Li, C.-W. Chu, V. Shrotriya, J. Huang, Y. Yang, *Appl. Phys. Lett.* 88 (2006) 253503.
- [17] C. Waldauf, M. Morana, P. Denk, P. Schilinsky, K. Coakley, S.A. Choulis, C.J. Brabec, *Appl. Phys. Lett.* 89 (2006) 233517.
- [18] S.K. Hau, H.L. Yip, H. Ma, A.K.-Y. Jen, *Appl. Phys. Lett.* 93 (2008) 233304.
- [19] T. Ameri, G. Dennler, C. Waldauf, P. Denk, K. Forberich, M.C. Scharber, C.J. Brabec, K. Hingerl, *J. Appl. Phys.* 103 (2008) 084506.
- [20] C.-H. Hsieh, Y.-J. Cheng, P.-J. Li, C.-H. Chen, M. Dubosc, R.-M. Liang, C.-S. Hsu, *J. Am. Chem. Soc.* 132 (2010) 4887.
- [21] T.B. Yang, W.Z. Cai, D.H. Qin, E.G. Wang, L.G. Lan, X. Gong, J.B. Peng, Y. Cao, *J. Phys. Chem. C* 114 (2010) 6849.
- [22] Y.M. Sun, J.H. Seo, C.J. Takacs, J. Seifter, A.J. Heeger, *Adv. Mater.* 23 (2011) 1679.
- [23] D. Baierl, B. Fabel, P. Gabos, P. Lucio, P. Lugli, G. Scarpa, *Org. Electron.* 11 (2010) 1199.
- [24] Ü. Özgür, Ya.I. Alivov, C. Liu, A. Teke, M.A. Reshchikov, S. Doğan, V. Avrutin, S.-J. Cho, H. Morkoç, *J. Appl. Phys.* 98 (2005) 041301.
- [25] V. Shrotriya, G. Li, Y. Yao, C.-W. Chu, Y. Yang, *Appl. Phys. Lett.* 88 (2006) 073508.
- [26] I. Hancox, K.V. Chauhan, P. Sullivan, R.A. Hatton, A. Moshar, C.P.A. Mulcahy, T.S. Jones, *Energy Environ. Sci.* 3 (2010) 107.
- [27] T. Stubhan, T. Ameri, M. Salinas, J. Krantz, F. Machui, M. Halik, C.J. Brabec, *Appl. Phys. Lett.* 98 (2011) 253308.

- [28] Y.M. Sun, C.J. Takacs, S.R. Cowan, J.H. Seo, X. Gong, A. Roy, A.J. Heeger, *Adv. Mater.* 23 (2011) 2226.
- [29] S. Murace, Y. Yang, *Adv. Mater.* 24 (2012) 2459.
- [30] M. Kröger, S. Hamwi, J. Meyer, T. Riedl, W. Kowalsky, A. Kahn, *Appl. Phys. Lett.* 95 (2009) 123301.
- [31] H. Hoppe, N.S. Sariciftci, *J. Mater. Chem.* 19 (2004) 1924.
- [32] S. Günes, H. Neugebauer, N.S. Sariciftci, *Chem. Rev.* 107 (2007) 1324.
- [33] L.-M. Chen, Z. Hong, G. Li, Y. Yang, *Adv. Mater.* 21 (2009) 1434.
- [34] D. Mühlbacher, M. Scharber, M. Morana, Z. Zhu, D. Waller, R. Gaudiana, C.J. Brabec, *Adv. Mater.* 18 (2006) 2884.
- [35] C. Soci, I.-W. Hwang, D. Moses, Z. Zhu, D. Waller, R. Gaudiana, C.J. Brabec, A.J. Heeger, *Adv. Funct. Mater.* 17 (2007) 632.
- [36] J. Peet, R.C. Coffin, T.Q. Nguyen, A. Mikhailovsky, D. Moses, G.C. Bazan, *Appl. Phys. Lett.* 89 (2006) 252105.
- [37] J. Peet, J.Y. Kim, N.E. Coates, W.L. Ma, D. Moses, A.J. Heeger, G.C. Bazan, *Nat. Mater.* 6 (2007) 497.
- [38] W. Ma, C. Yang, X. Gong, K. Lee, A.J. Heeger, *Adv. Funct. Mater.* 15 (2005) 1617.
- [39] T. Agostinelli, T.A.M. Ferenczi, E. Pires, S. Foster, A. Maurano, C. Müller, A. Ballantyne, M. Hampton, S. Lilliu, M. Campoy-Quiles, H. Azimi, M. Morana, D.D.C. Bradley, J. Durrant, J.E. Macdonald, N. Stingelin, J. Nelson, *J. Polym. Sci. Part B: Polym. Phys.* 49 (2011) 717.